HHS Public Access

Author manuscript

Science. Author manuscript; available in PMC 2018 November 18.

Published in final edited form as:

Science. 2018 May 18; 360(6390): 795–800. doi:10.1126/science.aaq0926.

Gut microbiota utilize immunoglobulin A for mucosal colonization

G.P. Donaldson[1,*], **M.S. Ladinsky**[1], **K.B. Yu**[1], **J.G. Sanders**[2], **B.B. Yoo**[1], **W.C. Chou**[3], **M.E. Conner**[4], **A.M. Earl**[3], **R. Knight**[2], **P.J. Bjorkman**[1], and **S.K. Mazmanian**[1,*]

[1]Department of Biology and Biological Engineering, California Institute of Technology, Pasadena, CA 91125, USA

[2]Deparment of Pediatrics, University of California, San Diego, California, 92110; Department of Computer Science and Engineering, University of California, San Diego, California, USA 92093

[3]Infectious Disease and Microbiome Program, Broad Institute of MIT and Harvard, Cambridge, MA 02142, USA

[4]Department of Molecular Virology and Microbiology, Baylor College of Medicine, Houston, TX 77030, USA

Abstract

The immune system responds vigorously to microbial infection, while permitting life-long colonization by the microbiome. Mechanisms that facilitate the establishment and stability of the gut microbiota remain poorly described. We discovered that a sensor/regulatory system in the prominent human commensal *Bacteroides fragilis* modulates its surface architecture to invite binding of immunoglobulin A (IgA). Specific immune recognition facilitated bacterial adherence to cultured intestinal epithelial cells and intimate association with the gut mucosal surface *in vivo*. The IgA response was required for *B. fragilis*, and other commensal species, to occupy a defined mucosal niche that mediated stable colonization of the gut through exclusion of exogenous competitors. Therefore, in addition to its role in pathogen clearance, we propose that IgA responses can be co-opted by the microbiome to engender robust host-microbial symbiosis.

Main Text

At birth, ecological and evolutionary processes commence to assemble a complex microbial consortium in the animal gut. Community composition of the adult human gut microbiome is remarkably stable during health, despite day-to-day variability in diet and diverse environmental exposures. Instability, or dysbiosis, may be involved in the etiology of a variety of immune, metabolic, and neurologic diseases (1, 2). Longitudinal sequencing studies indicate a majority of bacterial strains persist within an individual for years (3), and for most species there is a single, persistently dominant strain (4) (termed “single-strain stability”). Mucus and components of the innate and adaptive immune systems are thought to influence microbiome stability, independently of diet. For example, immunoglobulin A

*Correspondence to: gdonalds@caltech.edu and sarkis@caltech.edu.

(IgA), the main antibody isotype secreted in the gut, shapes the composition of the intestinal microbiome via currently unknown mechanisms (5–8). IgA deficiency in mice increases inter-individual variability in the microbiome (9) and decreases diversity (10, 11). The direct effects of IgA on bacteria have largely been studied in the context of enteric infection by pathogens (12). However, early studies of IgA in the healthy gut found that the majority of live bacterial cells in feces are bound by IgA (13), reflecting a steady-state IgA response to persistent indigenous microbes (14). Studies show that IgA promotes adherence of commensal bacteria to tissue-cultured intestinal epithelial cells (15, 16), though the *in vivo* implications of this observation are unclear. Furthermore, lack of IgA, the most common human immunodeficiency, does not affect lifespan and only modestly increases susceptibility to respiratory and gastrointestinal infections (17), raising the question of why the immune system evolved to invest the considerable energy to produce several grams of IgA daily (18).

Bacteroides fragilis is an important member of the human gut microbiome, with beneficial properties that ameliorate inflammatory and behavioral symptoms in preclinical animal models (19–22). This commensal exhibits remarkable single-strain stability (23, 24) and enriched colonization of the gut mucosal surface (25). To explore physical features of *B. fragilis* interaction with the host epithelium, we used transmission electron microscopy (TEM) to visualize colonic tissues of mono-colonized mice. *B. fragilis* commonly formed discrete aggregates of tightly-packed cells on the apical epithelial surface (Fig. 1A) and penetrated the glycocalyx layer of transmembrane mucins, nearly contacting the microvilli (Fig. 1B and fig. S1A and B). Intact *B. fragilis* cells were also found nestled in the ducts of the crypts of Lieberkühn (Fig. 1C and S1C). We previously identified a genetic locus in *B. fragilis*, named the *c*ommensal *c*olonization *f*actors (*ccfABCDE*), which is necessary for colonization of colonic crypts (26). To assess how these genes affect bacterial localization to the mucosal surface, we mono-colonized mice with a *ccfCDE* (Δ*ccf*) mutant. By TEM, *B. fragilis* Δ*ccf* was only found as sparse, individual cells within the epithelial mucosa, excluded from contact with the glycocalyx (Fig. 1D and E), and never observed in aggregates as for wild-type bacteria (Fig. 1F). *B. fragilis* burden in the colon lumen was identical between strains (fig. S2A), suggesting that the CCF system is required specifically for bacterial aggregation within mucus.

High-resolution tomograms of bacterial cells *in vivo* revealed the presence of a thick, fuzzy capsule layer covering wild-type *B. fragilis* (Fig. 1G), which was significantly reduced in *B. fragilis* Δ*ccf* (Fig. 1H and 1I). We sought to investigate the bacterial physiology underlying this ultrastructural change, and potential corresponding effects on colonization. The *ccf* locus is highly induced during gut colonization (26) and bacterial growth in mucin O-glycans (27), indicating the CCF system may sense a specific host-derived glycan. The *ccf* genes are homologous to polysaccharide utilization systems in which a sigma factor (*ccfA*) is activated by extracellular glycan sensing (28), thus we hypothesized that *ccfA* may activate genes involved in mucosal colonization. We overexpressed *ccfA* in *B. fragilis* and assessed global gene expression by RNAseq during *in vitro* growth (without overexpression *ccf* is poorly expressed in culture (26)). Of the non-*ccf* genes regulated by *ccfA*, 24 out of 25 genes mapped to the biosynthesis loci for capsular polysaccharides A and C (PSA and PSC) (Fig. 2A, 2B and Table S1). Correspondingly, *ccf* mutation decreased expression of PSC and

increased expression of PSA *in vivo* (Fig. 2C). While phase variation of capsular polysaccharides is known to influence general *in vivo* fitness of *B. fragilis* (29, 30), these studies identify a pathway for transcriptional regulation of specific polysaccharides in the context of mucosal colonization.

We modeled single-strain stability using a horizontal transmission assay, wherein co-housing animals respectively harboring isogenic strains of wild-type *B. fragilis* resulted in minimal strain transmission from one animal to another (Fig. 2D, S2A). This intra-species colonization resistance is provided through bacterial occupation of a species-specific nutrient or spatial niche (26). However, as previously reported (26), if mice are colonized initially with *B. fragilis* Δ*ccf*, animals were permissive to co-colonization by wild-type *B. fragilis* after co-housing (Fig. 2E, S2B), indicating a CCF-dependent defect in niche saturation. Mice harboring a mutant in the biosynthesis genes for PSC (ΔPSC) showed highly variable co-colonization by wild-type bacteria (Fig. 2F, S2C). Interestingly, we observed an unexpected increase in expression of the PSB biosynthesis genes in this mutant (Fig. 2H), which may compensate for the loss of PSC. We generated a strain defective in synthesizing both PSB and PSC (ΔPSB/C), and mice mono-associated with the double mutant were consistently unable to maintain colonization resistance (Fig. 2G, S2D–F), though the strain retained *ccf* expression (fig. S2G). Despite lack of competition in a mono-colonized setting and equal levels of colonization in the colon lumen (fig. S2H), the *B. fragilis* Δ*ccf* and ΔPSB/C strains were defective in colonization of the ascending colon mucus (Fig. 2I), reflecting impaired saturation of the mucosal niche. Accordingly, when we imaged the ΔPSB/C strain *in vivo* employing TEM, though the capsule was not as thin as in *B. fragilis* Δ*ccf* (fig. S2I and J), the hallmark epithelial aggregation phenotype was abrogated compared to wild-type bacteria (fig. S2K and L). Therefore, we conclude that the CCF system regulates capsule expression to mediate *B. fragilis* mucosal colonization and single strain stability.

To investigate host responses contributing to mucosal colonization, we defined the transcriptome of the ascending colon during colonization with wild-type *B. fragilis* or *B. fragilis* Δ*ccf*. Remarkably, 7 of the 14 differentially expressed genes encode immunoglobulin variable chains (Fig. 3A and table S2). We did not observe any elevation of immune responses in Δ*ccf*–colonized mice (fig. S3A), indicating that changes in mucosal association are not caused by inflammation. Accordingly, we tested whether capsular polysaccharide regulation by *ccf* affects IgA recognition of bacteria (31–33). In fecal samples from mono-colonized animals, wild-type *B. fragilis* was highly coated with IgA, which was significantly diminished in Δ*ccf* and ΔPSB/C strains (Fig. 3B, 3C, and S4A). We observed no difference between these strains in the induction of total fecal IgA (Fig. 3D), reflecting equivalent stimulation of nonspecific IgA production (10, 34, 35). To test bacteria-specific responses, IgA extracted from feces of mice mono-colonized with *B. fragilis* was evaluated for binding to bacteria recovered from mono-colonized *Rag1*$^{-/-}$ mice (*in vivo*-adapted, yet IgA-free bacteria). Western blots of bacterial lysates showed that strong IgA reactivity to capsular polysaccharides was abrogated in the Δ*ccf* and ΔPSB/C strains (Fig. 3E and F). Although IgA can be polyreactive (10, 34, 35), binding to lysates of *Bacteroides* was species-specific (fig. S4B) and required induction of IgA following bacterial colonization (fig. S4C and D). Accordingly, in a whole bacteria binding assay, IgA induced by wild-type bacteria

maximally coated wild-type *B. fragilis* compared with the Δ*ccf* and ΔPSB/C strains (Fig. 3G). IgA induced by *B. fragilis* Δ*ccf* exhibited reduced binding to wild-type bacteria (Fig. 3G). The addition of IgA to *in vivo*-adapted, IgA-free bacteria increased adherence of *B. fragilis* to intestinal epithelial cells in tissue culture (Fig. 3H), yet had no effect on bacterial viability (fig. S4E). Cell lines known to produce more mucus (36) exhibited a greater capacity for IgA-enhanced *B. fragilis* adherence (fig. S4F), consistent with prior work showing that IgA binds mucus (36–38). Importantly, IgA-enhanced adherence was decreased if targeted bacteria lack *ccf* or PSB/C, or if the IgA tested was induced by a *ccf* mutant or *Bacteroides thetaiotaomicron* (Fig. 3H and S4G). While pathogenic bacteria elaborate capsular polysaccharides for immune evasion, these results suggest *B. fragilis* deploys specific capsules for immune attraction, potentially enabling stable mucosal colonization.

We determined whether IgA coating promotes *B. fragilis* colonization in mice. Using the horizontal transmission paradigm, *Rag1*$^{-/-}$ mice colonized with wild-type *B. fragilis* were readily co-colonized by an isogenic strain from a co-housed animal (fig. S5A and B), showing loss of colonization resistance in the absence of adaptive immunity. We next treated wild-type mice with an anti-CD20 antibody (fig. S5C) (39) to deplete B cells (fig. S5D–F), thus reducing total fecal IgA levels (fig. S5G) and eliminating IgA coating of wild-type *B. fragilis* during mono-colonization (Fig. 4A). IgA recovered from isotype control treated mice, also mono-colonized with *B. fragilis*, promoted adherence of wild-type bacteria to epithelial cells *in vitro*, while IgA from anti-CD20 treated mice had no effect despite being exposed to *B. fragilis* antigens (Fig. 4B). In the horizontal transmission assay, B cell depleted mice mono-colonized with *B. fragilis* were readily invaded by wild-type bacteria, while isotype control-injected animals retained colonization resistance (Fig. 4C and S5H). Therefore, active B cell responses to *B. fragilis* colonization enhance single-strain stability.

As B cell depletion eliminates all antibody isotypes, germ-free IgA$^{-/-}$ mice (40) were generated and mono-colonized with *B. fragilis*. We did not observe compensatory coating by IgM (fig. S6A). In a horizontal transmission assay with wild-type (BALB/c) and IgA$^{-/-}$ mice, lack of IgA allowed co-colonization by challenge strains (Fig. 4D, S6B–D), indicating that IgA specifically contributes to single-strain stability. This feature was reproduced in mice with a full microbial community “spiked” with genetically marked *B. fragilis* strains (fig. S6E and F), revealing that single-strain stability of an individual bacterial species occurs in the context of a complex community. Mono-colonized IgA$^{-/-}$ mice harbored reduced levels of live bacteria in the colon mucus compared to wild-type mice (Fig. 4E), though they had greater numbers of bacteria in the colon lumen (fig. S6G). TEM images of ascending colon tissues reveal that in IgA$^{-/-}$ animals, wild-type *B. fragilis* failed to aggregate on the epithelial surface (Fig. 4F and 4G), similar to the *ccf* and PSB/C mutants in wild-type animals. *B. fragilis* cells also formed aggregates in feces in the presence of IgA (fig. S7), indicating that enhanced mucosal colonization may be due to increased aggregation or growth (41) within mucus. These findings converge to support a model whereby *ccf* regulates expression of specific capsular polysaccharides to attract IgA binding, allowing for robust mucosal colonization and single-strain stability.

Beyond *B. fragilis*, we tested whether IgA shapes a complex microbiome following controlled introduction of mouse microbiota to germ-free BALB/c or $IgA^{-/-}$ mice. One month following colonization, despite similar microbiome profiles in feces of both mouse genotypes (fig. S8A), we observed differences for specific taxa (Table S3). We also identified a defect in community stratification between the colonic mucus and lumen of $IgA^{-/-}$ mice (Fig. 4H and S8B), revealing that IgA is required to individualize microbiome profiles between these two anatomic locations. Remarkably, a highly mucus-enriched exact sequence variant (ESV), mapping uniquely to *B. fragilis*, was significantly decreased in the mucus of $IgA^{-/-}$ mice compared to BALB/c mice (Fig. 4I and S9A), naturally supporting our observations from mono-colonized mice. To extend this analysis to other microbial species, we identified Rikanellaceae, *Blautia sp.*, and segmented filamentous bacteria (SFB) as being highly IgA-coated (fig. S9B) (35), and assessed the abundance of these taxa in the colonic or ileal mucus. *Blautia sp.* and segmented filamentous bacteria (SFB) displayed increased mucosal association in the absence of IgA (Fig. 4I) (42), demonstrating that IgA can protect the intestinal barrier. However, similar to *B. fragilis*, Rikanellaceae were highly abundant in colon mucus and significantly depleted in $IgA^{-/-}$ mice (Fig. 4I). We conclude that IgA-enhanced mucosal colonization occurs within complex communities for multiple strains of *B. fragilis* and other species of the gut microbiome.

Classically viewed, the immune system evolved to prevent microbial colonization. However, not only do animals tolerate a complex microbiome, in the case of *B. fragilis* provoking an immune response paradoxically enables intimate association with its mammalian host. Related commensal bacteria may also benefit from actively engaging IgA during symbiosis, as $Rag2^{-/-}$ mice devoid of adaptive immunity harbor fewer *Bacteroides* (43), and both B cell deficient and $IgA^{-/-}$ animals display decreased colonization by the Bacteroidaceae family (44). IgA has been previously shown to increase adherence of *Escherichia coli* (15), *Bifidobacterium lactis,* and *Lactobacillus ramnosus* (16) to tissue-cultured epithelial cells, suggesting that these microorganisms may also benefit from IgA to establish a mucosal bacterial community. Mucosal microbiome instability or loss of immunomodulatory species may underlie the link between IgA deficiency and autoimmune diseases in humans (45). Interestingly, while IgA-coated bacteria from individuals with IBD (46) or nutritional deficiencies (47) exacerbate respective pathologies in mice, IgA-coated bacteria from healthy humans protect mice from disease (47). We propose that during health, IgA fosters mucosal colonization of microbiota with beneficial properties (9), while disease states may induce (or be caused by) IgA responses to pathogens or pathobionts that disrupt healthy microbiome equilibria. Indeed, computational models indicate that IgA can both maintain indigenous mucosal populations and clear invasive pathogens (48). In addition to serving as a defense system, we discover that adaptive immunity evolved to engender intimate association with members of the gut microbiome.

Supplementary Material

Refer to Web version on PubMed Central for supplementary material.

Acknowledgments

We thank Drs. Elaine Hsiao, June Round, Hiutung Chu, and members of the Mazmanian laboratory for critical review of this manuscript. The anti-CD20 antibody was provided under an MTA from Genentech. We appreciate technical support from Taren Thron, the Caltech Office of Laboratory Animal Resources, Caltech Genomics Laboratory, and Caltech Flow Cytometry Facility. G.P.D. was supported by an NIH training grant (5T32 GM07616) and NSF Graduate Research Fellowship (DGE-1144469). Support for this research was provided by grants from the National Institutes of Health to the Broad Institute (U19AI110818), the NIH (P50 GM082545 and AI04123) to P.B.J., the NIH (GM099535 and DK083633) to S.K.M., and the Heritage Medical Research Institute to S.K.M. All data and code to understand and assess the conclusions of this research are available in the main text, supplementary materials and via the following repositories: EMBL-EBI accession ERP107727 and NCBI Bioproject accessions PRJNA445716 and PRJNA438372.

References and Notes

1. Hall AB, Tolonen AC, Xavier RJ. Human genetic variation and the gut microbiome in disease. Nat Rev Genet. 2017; doi: 10.1038/nrg.2017.63
2. Fung TC, Olson CA, Hsiao EY. Interactions between the microbiota, immune and nervous systems in health and disease. Nat Neurosci. 2017; 20:145–155. [PubMed: 28092661]
3. Faith JJ, et al. The long-term stability of the human gut microbiota. Science. 2013; 341:1237439. [PubMed: 23828941]
4. Truong DT, Tett A, Pasolli E, Huttenhower C, Segata N. Microbial strain-level population structure and genetic diversity from metagenomes. Genome Res. 2017 gr.216242.116.
5. Fagarasan S, et al. Critical roles of activation-induced cytidine deaminase in the homeostasis of gut flora. Science. 2002; 298:1424–1427. [PubMed: 12434060]
6. Kawamoto S, et al. The inhibitory receptor PD-1 regulates IgA selection and bacterial composition in the gut. Science. 2012; 336:485–489. [PubMed: 22539724]
7. Macpherson AJ, Köller Y, McCoy KD. The bilateral responsiveness between intestinal microbes and IgA. Trends Immunol. 2015; 36:460–470. [PubMed: 26169256]
8. Kubinak JL, Round JL. Do antibodies select a healthy microbiota? Nat Rev Immunol. 2016; 16:767–774. [PubMed: 27818504]
9. Kubinak JL, et al. MyD88 signaling in T cells directs IgA-mediated control of the microbiota to promote health. Cell Host Microbe. 2015; 17:153–163. [PubMed: 25620548]
10. Fransen F, et al. BALB/c and C57BL/6 Mice Differ in Polyreactive IgA Abundance, which Impacts the Generation of Antigen-Specific IgA and Microbiota Diversity. Immunology. 2015; 43:527–540.
11. Kawamoto S, et al. Foxp3(+) T cells regulate immunoglobulin a selection and facilitate diversification of bacterial species responsible for immune homeostasis. Immunology. 2014; 41:152–165.
12. Mantis NJ, Forbes SJ. Secretory IgA: arresting microbial pathogens at epithelial borders. Immunol Invest. 2010; 39:383–406. [PubMed: 20450284]
13. van der Waaij LA, Limburg PC, Mesander G, van der Waaij D. In vivo IgA coating of anaerobic bacteria in human faeces. Gut. 1996; 38:348–354. [PubMed: 8675085]
14. Shroff KE, Meslin K, Cebra JJ. Commensal enteric bacteria engender a self-limiting humoral mucosal immune response while permanently colonizing the gut. Infect Immun. 1995; 63:3904–3913. [PubMed: 7558298]
15. Bollinger RR, et al. Human secretory immunoglobulin A may contribute to biofilm formation in the gut. Immunology. 2003; 109:580–587. [PubMed: 12871226]
16. Mathias A, et al. Potentiation of polarized intestinal Caco-2 cell responsiveness to probiotics complexed with secretory IgA. J Biol Chem. 2010; 285:33906–33913. [PubMed: 20729211]
17. Yel L. Selective IgA deficiency. Journal of clinical immunology. 2010; doi: 10.1007/s10875-009-9357-x
18. Conley ME. D. D. A. O. I. medicine. Intravascular and mucosal immunoglobulin A: two separate but related systems of immune defense? Am Coll Physicians. 1987; doi: 10.7326/0003-4819-106-6-892

19. Mazmanian SK, Round JL, Kasper DL. A microbial symbiosis factor prevents intestinal inflammatory disease. Nature. 2008; 453:620–625. [PubMed: 18509436]
20. Ochoa-Repáraz J, et al. Central nervous system demyelinating disease protection by the human commensal Bacteroides fragilis depends on polysaccharide A expression. J Immunol. 2010; 185:4101–4108. [PubMed: 20817872]
21. Hsiao EY, et al. Microbiota modulate behavioral and physiological abnormalities associated with neurodevelopmental disorders. Cell. 2013; 155:1451–1463. [PubMed: 24315484]
22. Chu H, et al. Gene-microbiota interactions contribute to the pathogenesis of inflammatory bowel disease. Science. 2016; 352:1116–1120. [PubMed: 27230380]
23. Scholz M, et al. Strain-level microbial epidemiology and population genomics from shotgun metagenomics. Nat Methods. 2016; 13:435–438. [PubMed: 26999001]
24. Yassour M, et al. Natural history of the infant gut microbiome and impact of antibiotic treatment on bacterial strain diversity and stability. Science Translational Medicine. 2016; 8:343ra81–343ra81.
25. Yasuda K, et al. Biogeography of the intestinal mucosal and lumenal microbiome in the rhesus macaque. Cell Host Microbe. 2015; 17:385–391. [PubMed: 25732063]
26. Lee SM, et al. Bacterial colonization factors control specificity and stability of the gut microbiota. Nature. 2013; 501:426–429. [PubMed: 23955152]
27. Pudlo NA, et al. Symbiotic Human Gut Bacteria with Variable Metabolic Priorities for Host Mucosal Glycans. MBio. 2015; 6doi: 10.1128/mBio.01282-15
28. Martens EC, Roth R, Heuser JE, Gordon JI. Coordinate regulation of glycan degradation and polysaccharide capsule biosynthesis by a prominent human gut symbiont. J Biol Chem. 2009; 284:18445–18457. [PubMed: 19403529]
29. Coyne MJ, Chatzidaki-Livanis M, Paoletti LC, Comstock LE. Role of glycan synthesis in colonization of the mammalian gut by the bacterial symbiont Bacteroides fragilis. Proc Natl Acad Sci USA. 2008; 105:13099–13104. [PubMed: 18723678]
30. Liu CH, Lee SM, Vanlare JM, Kasper DL, Mazmanian SK. Regulation of surface architecture by symbiotic bacteria mediates host colonization. Proc Natl Acad Sci USA. 2008; 105:3951–3956. [PubMed: 18319345]
31. Peterson DA, McNulty NP, Guruge JL, Gordon JI. IgA response to symbiotic bacteria as a mediator of gut homeostasis. Cell Host Microbe. 2007; 2:328–339. [PubMed: 18005754]
32. Zitomersky NL, Coyne MJ, Comstock LE. Longitudinal analysis of the prevalence, maintenance, and IgA response to species of the order Bacteroidales in the human gut. Infect Immun. 2011; 79:2012–2020. [PubMed: 21402766]
33. Moor K, et al. Analysis of bacterial-surface-specific antibodies in body fluids using bacterial flow cytometry. Nat Protoc. 2016; 11:1531–1553. [PubMed: 27466712]
34. Shimoda M, Inoue Y, Azuma N, Kanno C. Natural polyreactive immunoglobulin A antibodies produced in mouse Peyer's patches. Immunology. 1999; 97:9–17. [PubMed: 10447709]
35. Bunker JJ, et al. Natural polyreactive IgA antibodies coat the intestinal microbiota. Science. 2017; 358:eaan6619. [PubMed: 28971969]
36. Gibbins HL, Proctor GB, Yakubov GE, Wilson S, Carpenter GH. SIgA binding to mucosal surfaces is mediated by mucin-mucin interactions. PLoS ONE. 2015; 10:e0119677. [PubMed: 25793390]
37. Biesbrock AR, Reddy MS, Levine MJ. Interaction of a salivary mucin-secretory immunoglobulin A complex with mucosal pathogens. Infect Immun. 1991; 59:3492–3497. [PubMed: 1910004]
38. Phalipon A, et al. Secretory component: a new role in secretory IgA-mediated immune exclusion in vivo. Immunology. 2002; 17:107–115.
39. Sarikonda G, et al. Transient B-cell depletion with anti-CD20 in combination with proinsulin DNA vaccine or oral insulin: immunologic effects and efficacy in NOD mice. PLoS ONE. 2013; 8:e54712. [PubMed: 23405091]
40. Blutt SE, Miller AD, Salmon SL, Metzger DW, Conner ME. IgA is important for clearance and critical for protection from rotavirus infection. Mucosal Immunol. 2012; 5:712–719. [PubMed: 22739233]
41. Moor K, et al. High-avidity IgA protects the intestine by enchaining growing bacteria. Nature. 2017; 103:3–19.

42. Suzuki K, et al. Aberrant expansion of segmented filamentous bacteria in IgA-deficient gut. Proc Natl Acad Sci USA. 2004; 101:1981–1986. [PubMed: 14766966]
43. Barroso-Batista J, Demengeot J, Gordo I. Adaptive immunity increases the pace and predictability of evolutionary change in commensal gut bacteria. Nat Commun. 2015; 6:8945. [PubMed: 26615893]
44. Mirpuri J, et al. Proteobacteria-specific IgA regulates maturation of the intestinal microbiota. Gut Microbes. 2014; 5:28–39. [PubMed: 24637807]
45. Singh K, Chang C, Gershwin ME. IgA deficiency and autoimmunity. Autoimmun Rev. 2014; 13:163–177. [PubMed: 24157629]
46. Palm NW, et al. Immunoglobulin A coating identifies colitogenic bacteria in inflammatory bowel disease. Cell. 2014; 158:1000–1010. [PubMed: 25171403]
47. Kau AL, et al. Functional characterization of IgA-targeted bacterial taxa from undernourished Malawian children that produce diet-dependent enteropathy. Science Translational Medicine. 2015; 7:276ra24–276ra24.
48. McLoughlin K, Schluter J, Rakoff-Nahoum S, Smith AL, Foster KR. Host Selection of Microbiota via Differential Adhesion. Cell Host Microbe. 2016; 19:550–559. [PubMed: 27053168]
49. Mastronarde DN. Automated electron microscope tomography using robust prediction of specimen movements. J Struct Biol. 2005; 152:36–51. [PubMed: 16182563]
50. Kremer JR, Mastronarde DN, McIntosh JR. Computer visualization of three-dimensional image data using IMOD. J Struct Biol. 1996; 116:71–76. [PubMed: 8742726]
51. Mastronarde DN. Correction for non-perpendicularity of beam and tilt axis in tomographic reconstructions with the IMOD package. J Microsc. 2008; 230:212–217. [PubMed: 18445149]
52. McClure R, et al. Computational analysis of bacterial RNA-Seq data. Nucleic Acids Res. 2013; 41:e140. [PubMed: 23716638]
53. Dobin A, et al. STAR: ultrafast universal RNA-seq aligner. Bioinformatics. 2013; 29:15–21. [PubMed: 23104886]
54. Anders S, Pyl PT, Huber W. HTSeq--a Python framework to work with high-throughput sequencing data. Bioinformatics. 2015; 31:166–169. [PubMed: 25260700]
55. Robinson MD, McCarthy DJ, Smyth GK. edgeR: a Bioconductor package for differential expression analysis of digital gene expression data. Bioinformatics. 2010; 26:139–140. [PubMed: 19910308]
56. Caporaso JG, et al. Ultra-high-throughput microbial community analysis on the Illumina HiSeq and MiSeq platforms. ISME J. 2012; 6:1621–1624. [PubMed: 22402401]
57. Thompson LR, et al. A communal catalogue reveals Earth's multiscale microbial diversity. Nature. 2017; 551:457–463. [PubMed: 29088705]
58. Amir A, et al. Deblur Rapidly Resolves Single-Nucleotide Community Sequence Patterns. mSystems. 2017; 2doi: 10.1128/mSystems.00191-16
59. DeSantis TZ, et al. Greengenes, a chimera-checked 16S rRNA gene database and workbench compatible with ARB. Applied and Environmental Microbiology. 2006; 72:5069–5072. [PubMed: 16820507]
60. Mirarab S, Nguyen N, Warnow T. SEPP: SATé-enabled phylogenetic placement. Pac Symp Biocomput. 2012:247–258. [PubMed: 22174280]
61. Paulson JN, Stine OC, Bravo HC, Pop M. Differential abundance analysis for microbial marker-gene surveys. Nat Methods. 2013; 10:1200–1202. [PubMed: 24076764]
62. Love MI, Huber W, Anders S. Moderated estimation of fold change and dispersion for RNA-seq data with DESeq2. Genome Biol. 2014; 15:550. [PubMed: 25516281]
63. R. C. Team. R: A language and environment for statistical computing. 2013
64. Lozupone C, Knight R. UniFrac: a new phylogenetic method for comparing microbial communities. Applied and Environmental Microbiology. 2005; 71:8228–8235. [PubMed: 16332807]
65. Anderson MJ. A new method for non−parametric multivariate analysis of variance. Austral Ecology. 2001; 26:32–46.

66. Oksanen, J., Kindt, R., Legendre, P., O'Hara, B. The Vegan Package—Community Ecology Package. 2007. R package version 2.0-9

67. Coyne MJ, Kalka-Moll W, Tzianabos AO, Kasper DL, Comstock LE. Bacteroides fragilis NCTC9343 produces at least three distinct capsular polysaccharides: cloning, characterization, and reassignment of polysaccharide B and C biosynthesis loci. Infect Immun. 2000; 68:6176–6181. [PubMed: 11035722]

68. Smith CJ, Rogers MB, McKee ML. Heterologous gene expression in Bacteroides fragilis. Plasmid. 1992; 27:141–154. [PubMed: 1615064]

69. Stevens AM, Shoemaker NB, Salyers AA. The region of a Bacteroides conjugal chromosomal tetracycline resistance element which is responsible for production of plasmidlike forms from unlinked chromosomal DNA might also be involved in transfer of the element. Journal of Bacteriology. 1990; 172:4271–4279. [PubMed: 2165473]

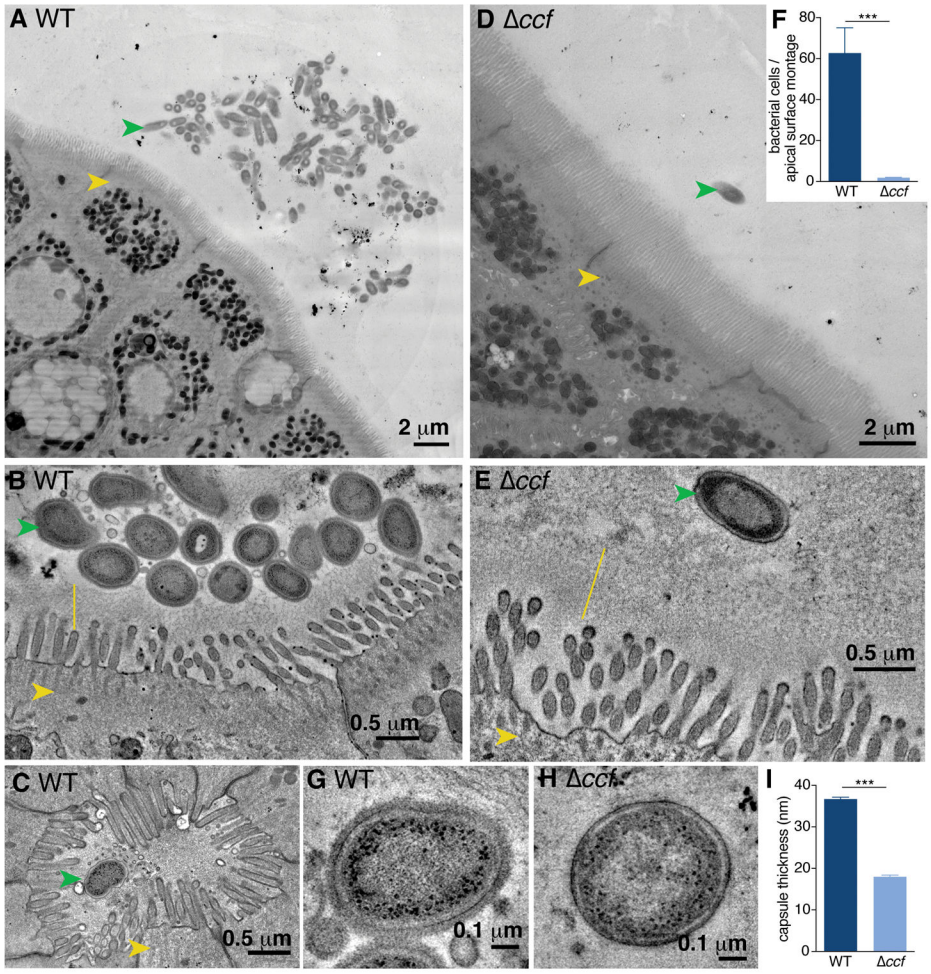

Fig. 1. *Bacteroides fragilis* resides as aggregates on the colon epithelium in a CCF-dependent manner

(**A**) Representative transmission electron microscopy (TEM) projection and (**B**) high-resolution tomogram of epithelial-associated wild-type *B. fragilis* in mono-colonized mice. Ascending colons of mice harbored aggregates of *B. fragilis* (green arrow) under non-pathogenic conditions, that made tight associations with the glycocalyx (yellow line) overlying intestinal epithelial cells (IECs, yellow arrow). (**C**) Tomogram of wild-type *B. fragilis* penetrating deep into the duct of a crypt of Lieberkühn. (**D**) Representative TEM projection image and (**E**) tomogram of epithelial-associated *B. fragilis* Δ*ccf.* The absence of the CCF system abrogated formation of bacterial aggregates and prevented intimate association with the glycocalyx. (n = 3 mice per group, about 1 mm epithelium scanned per mouse). (**F**) Quantification of bacterial cells per projection montage (A and D) of epithelial-associated bacteria (unpaired t test, n = 7, 8 images from 4 mice per group). (**G** and **H**) Tomogram of the bacterial surface of wild-type *B. fragilis* (G) in comparison to *B. fragilis* Δ*ccf* (H) revealed a thick fuzzy capsule for wild-type bacteria residing in the colons of mice. (**I**) Measurement of capsule thickness (unpaired t test, n = 10 cells from 3 mice per group) (*** $p < 0.001$).

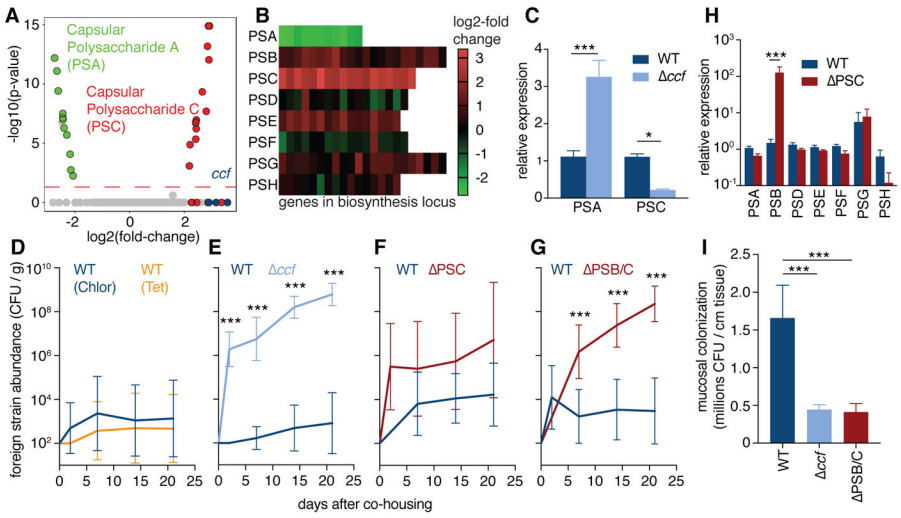

Fig. 2. Specific capsular polysaccharides, regulated by *ccf*, are necessary for single-strain stability

(**A**) RNAseq gene expression analysis of *B. fragilis* overexpressing *ccfA* during laboratory culture growth, relative to empty vector control (n = 3). Green symbols represent PSA genes; red symbols represent PSC genes; blue symbols represent *ccf* genes. (**B**) Heat map of expression levels for all capsular polysaccharide loci in *B. fragilis* following *ccfA* overexpression during growth in culture. (**C**) Relative expression using qRT-PCR (ΔΔCt normalized to gyrase) of RNA from colon lumen contents of mice mono-colonized with *B. fragilis* or *B. fragilis* Δ*ccf* (Sidak 2-way ANOVA, n = 4). (**D–G**) Abundance of foreign strains exchanged between pairs of co-housed mice each mono-colonized with the indicated strains, in colony forming units (CFU) per gram of feces (Sidak repeated measure 2-way ANOVA on log-transformed data, geometric mean and 95% CI, n = 9–12 pairs per plot). (**H**) Relative expression levels of capsular polysaccharides analyzed by qRT-PCR (ΔΔCt normalized to gyrase) of RNA from colon lumen contents of mice mono-colonized with *B. fragilis* or *B. fragilis* ΔPSC (Sidak 2-way ANOVA, n = 3, 4). (**I**) Plating of CFU from ascending colon mucus of mice mono-colonized with *B. fragilis* strains (Tukey ANOVA, n = 8) (* $p < 0.05$, ** $p < 0.01$, *** $p < 0.001$).

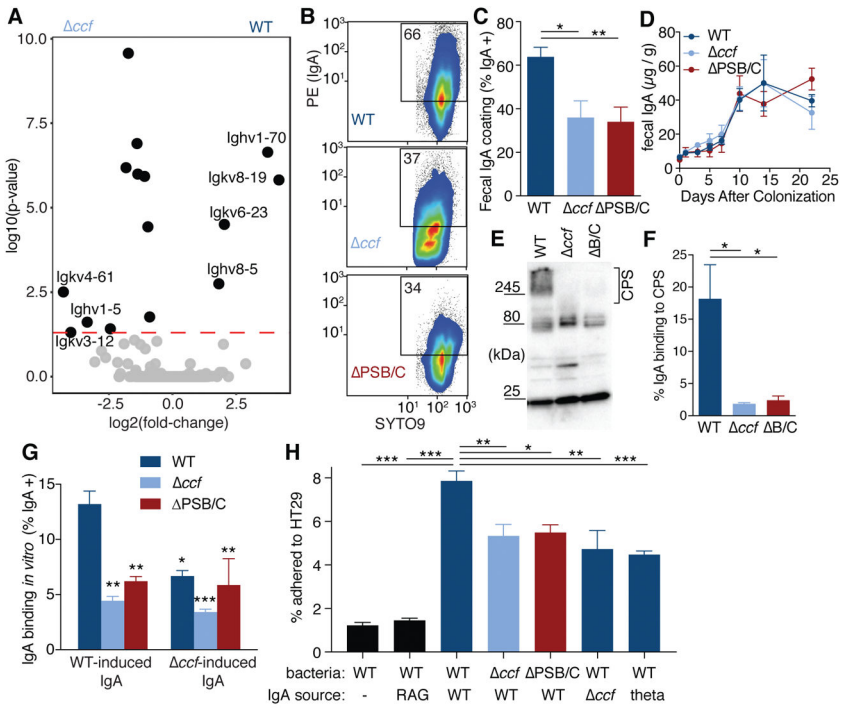

Fig. 3. *B. fragilis* induces a specific IgA response, dependent on *ccf* regulation of surface capsular polysaccharides, which enhances epithelial adherence

(**A**) RNAseq gene expression analysis of RNA recovered from whole ascending colon tissue of mice mono-colonized with *B. fragilis* or *B. fragilis* Δ*ccf* (n = 3). (**B**) Flow cytometry plots and (**C**) quantification of IgA coating of *B. fragilis* from feces of mice mono-colonized with various strains (Tukey ANOVA, n = 11–12). (**D**) ELISA for total fecal IgA in mono-colonized mice (Sidak repeated measure 2-way ANOVA, not significant, n = 4). (**E**) Bacterial lysates from feces of mono-colonized *Rag1*$^{-/-}$ mice probed in Western blots with fecal IgA from *B. fragilis* mono-colonized mice and (**F**) quantification of the proportional signal from IgA binding to capsular polysaccharides (CPS) (over 245 kDa) (Tukey ANOVA, n = 3 mice). (**G**) Binding of fecal IgA extracted from mono-colonized mice to various strains of *B. fragilis*. Source of IgA is mice colonized with either WT *B. fragilis* or *B. fragilis* Δ*ccf*. Because *ccf* is expressed *in vivo*, IgA-free bacteria from feces of mono-colonized *Rag1*$^{-/-}$ mice were used as the target for IgA binding (Tukey 2-way ANOVA, *significantly different from WT bacteria with WT IgA, n = 3). (**H**) *In vitro* epithelial cell adherence assay using IgA extracted from Swiss Webster mice (or *Rag1*$^{-/-}$, second column) mono-colonized with *B. fragilis* or *B. thetaiotaomicron* (theta; last column). IgA-free but *in vivo*-adapted bacteria were isolated from mono-colonized *Rag1*$^{-/-}$ mice (Tukey ANOVA, n = 4 mice as the source of bacteria) (* $p < 0.05$, ** $p < 0.01$, *** $p < 0.001$).

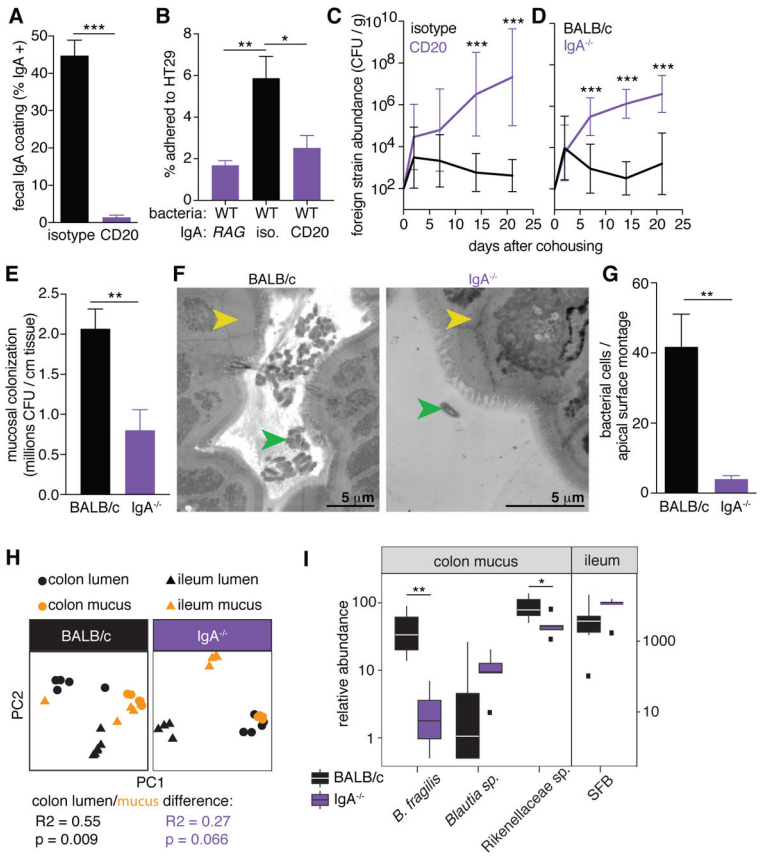

Fig. 4. IgA production *in vivo* is necessary for single-strain stability, mucosal colonization, and epithelial aggregation

(**A**) IgA coating of wild-type *B. fragilis* in feces following injection of anti-CD20 or isotype control antibody (unpaired t test, n = 8). (**B**) Epithelial cell adherence assay of wild-type *B. fragilis* incubated with IgA extracted from indicated mono-colonized mice (Tukey ANOVA, n = 4 mice as the source of bacteria). (**C**) Abundance of foreign strains exchanged between pairs of wild-type *B. fragilis* mono-colonized mice treated with anti-CD20 or an isotype control (Sidak repeated measure 2-way ANOVA on log-transformed data, n = 10). (**D**) Foreign strains exchanged between pairs of BALB/c and BALB/c IgA$^{-/-}$ mice mono-colonized with wild-type *B. fragilis* (Sidak repeated measure 2-way ANOVA on log-transformed data, n = 9). (**E**) CFU plating of ascending colon mucus of wild-type and IgA$^{-/-}$ mice mono-colonized with wild-type *B. fragilis* (unpaired t test, n = 9). (**F**) Representative TEM projections of ascending colon (yellow arrow: epithelial cell) from mice mono-colonized with wild-type *B. fragilis* (green arrow) (n = 3 mice per group, about 1 mm epithelium scanned per mouse) and (**G**) quantification of bacterial cells per projection montage (unpaired t test, n = 7, 6 images from 3 mice per group) (**H**) Principle coordinate analyses of weighed UniFrac distances of 16S community profiles of ex-germ-free BALB/c and BALB/c IgA$^{-/-}$ mice transplanted with a complex mouse microbiota (Adonis test within colon for lumen/mucus difference). (**I**) Relative abundance of *B. fragilis* and highly IgA-coated ESVs in ex-germ-free mice (* $p < 0.05$, ** $p < 0.01$, *** $p < 0.001$).